Eur. Phys. J. C (2023) 83:87
https://doi.org/10.1140/epjc/s10052-023-11230-6

THE EUROPEAN PHYSICAL JOURNAL C

Regular Article - Theoretical Physics

The LARES 2 satellite, general relativity and fundamental physics

Ignazio Ciufolini[2,1,a], **Antonio Paolozzi**[2], **Erricos C. Pavlis**[3], **John C. Ries**[4], **Richard Matzner**[5], **Claudio Paris**[2], **Emiliano Ortore**[2], **Vahe Gurzadyan**[6], **Roger Penrose**[7]

[1] Centro Fermi, Rome, Italy
[2] Scuola di Ingegneria Aerospaziale, Sapienza Università di Roma, Rome, Italy
[3] Goddard Earth Sciences Technology and Research II (GESTAR II), University of Maryland, Baltimore County, USA
[4] Center for Space Research, University of Texas at Austin, Austin, USA
[5] Center for Gravitational Physics, Weinberg Theory Center, University of Texas at Austin, Austin, USA
[6] Center for Cosmology and Astrophysics, Alikhanian National Laboratory, Yerevan State University, Yerevan, Armenia
[7] Mathematical Institute, University of Oxford, Oxford, UK

Received: 2 November 2022 / Accepted: 17 January 2023 / Published online: 30 January 2023

Abstract LARES 2, successfully launched on July 13, 2022, is a new generation laser-ranged satellite. LARES is an acronym for LAser RElativity Satellite. The first LARES satellite was successfully launched on February 13, 2012 with the ESA-ASI-AVIO launch vehicle VEGA. LARES 2 was injected with extremely high precision onto a high-altitude orbit at about 5900 km altitude with the new ESA-ASI-AVIO launch vehicle VEGA C. Laser-ranged satellites have many applications, including to test Einstein's theory of general relativity. The main general relativistic phenomenon that LARES 2 will test with high accuracy is the dragging of inertial frames, or frame-dragging. It will also test other aspects and principles of fundamental physics and general relativity, such as the weak equivalence principle at the foundation of viable gravitational theories. Frame-dragging is the name Einstein himself gave in 1913 to an intriguing phenomenon of general relativity which implies that a current of mass-energy, such as the rotation of a body, will generate spacetime curvature. Frame-dragging has a key role in high energy astrophysics, e.g., in the generation of gravitational waves by the collision of two black holes to form a rotating black hole. Frame-dragging by the rotating Earth was measured to a few percent accuracy by combining the data of the satellites LARES, LAGEOS and LAGEOS 2 (Ciufolini et al. in Eur Phys J C 79:872, 2019). LARES 2, thanks to its extremely high injection precision, is projected to improve the test of frame-dragging by at least an order of magnitude. LARES 2 has also relevant applications in space geodesy and geodynamics, e.g., in the study of the shape of the Earth and in the determination of the International Terrestrial Reference Frame (ITRF) by improving the determination of the Earth center of mass and by contributing to a better determination of its rotation axis.

1 The LARES 2 launch and its orbit

On July 13, 2022, at 13:13:17 UTC, the LARES 2 satellite (Fig. 1) was successfully launched from the ESA spaceport at Kourou in French Guyana aboard the validation flight of VEGA C, the new ESA-ASI-AVIO launch vehicle. About one hour later LARES 2 reached its orbit at about 5900 km altitude (see Table 1) with an exceptional injection precision, much better than what was required.

The LARES 2 orbital elements [1–4] are the same as those of a previously proposed (but never launched) satellite called LAGEOS 3 [5–11], in particular it has the same orbital inclination I (the angle between its orbital plane and the Earth's equatorial plane) and semimajor axis. However, the LARES 2 satellite has a structure substantially improved over that of LAGEOS 3 (Sect. 5), with a smaller ratio of cross-sectional-area to mass to minimize its non-gravitational orbital perturbations, and a special distribution of smaller retroreflectors which allows measuring its distance from laser-ranging stations on Earth with much higher precision.

The LARES 2 orbital inclination was proposed [1–11] to be supplementary to that of LAGEOS ($I_{Lageos} + I_{Lares2} = 180°$) in order to eliminate the effect of errors in modeling the secular shift of their nodes due to the non-sphericity of the Earth's shape and its gravitational field [12]. LAGEOS (Laser Geodynamic Satellite) is a NASA laser-ranged satellite launched in 1976 for space geodesy and geodynamics

[a] e-mail: ignazio.ciufolini@gmail.com (corresponding author)

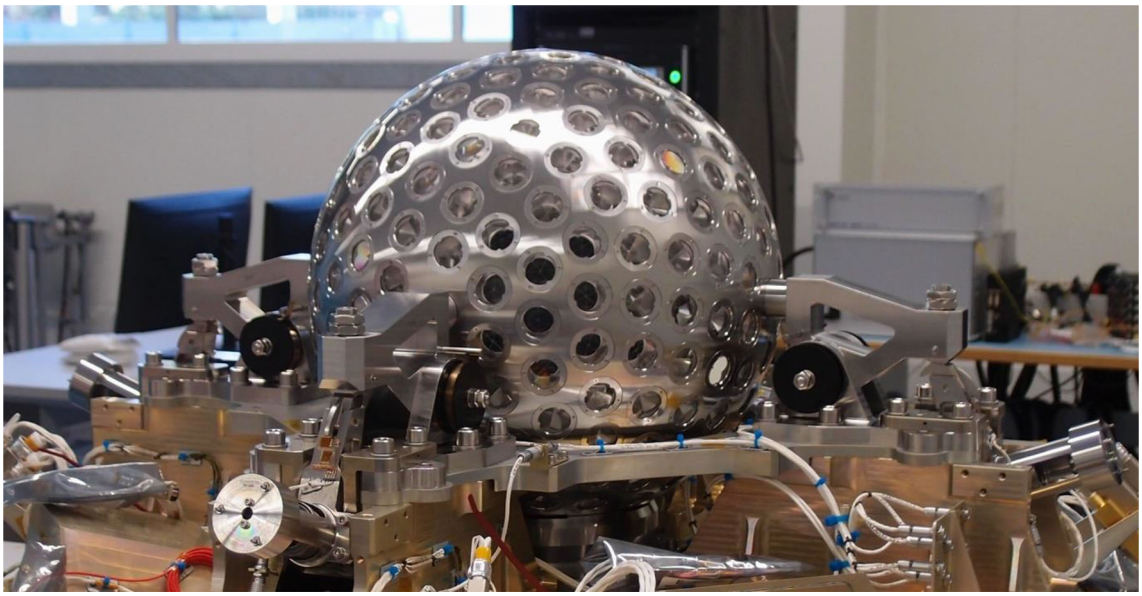

Fig. 1 The LARES 2 satellite before the launch mounted on the separation system

determinations. Since LAGEOS is a passive satellite, it is today still successfully tracked by the stations of the International Laser-Ranging Service (ILRS) [13].

The accuracy of the measurement of frame-dragging with two satellites depends on how precisely the orbital inclinations of the two satellites are supplementary and on how close their semimajor axes are equal, to allow the elimination of the bias due to the non-spherical Earth gravitational field (see Sect. 4).

In [1], we calculated the error in the measurement of frame-dragging due to any deviation of the orbit of LARES 2 from being perfectly matched in radius and perfectly supplementary in inclination to LAGEOS. A difference from supplementary of 0.15° in the inclination implies an error of about 10^{-3} in the measurement of frame-dragging and a difference of 20 km in the semimajor axis between the two satellites implies an error of about 10^{-3} in the measurement of frame-dragging.

By analyzing the first 127 days of LARES 2 laser-ranging data with the orbital estimators GEODYN and UTOPIA and the corresponding 127 days of laser-ranging data of LAGEOS, we found the *mean* orbital elements reported in Table 1. To compare the satellite's inclinations, we also fitted the inclinations with a quadratic polynomial where the epoch was about the mid-point of the time series. At the mid point, the inclination of LAGEOS 1 was 109.844° and LARES2 was 70.158° , with a good agreement with their mean calculated over the first 127 days. In the first row, we report the orbital inclination, semimajor axis and eccentricity of LARES 2, averaged over the first 127 days of daily estimations. In the second row the corresponding orbital elements of LAGEOS, in the third row the difference from 180° of the sum of their orbital inclinations and the difference in their semimajor axes. In the fourth row, we report the estimated error due to the deviation of the two orbits from being perfectly supplementary. We emphasize that other errors due to the non-static Earth gravitational field and to non-gravitational perturbations (see Sect. 4) must also be taken into account [1–11].

2 Tests of General Relativity and fundamental physics

Einstein's gravitational theory of General Relativity (GR) [14–16] has had a number of experimental and theoretical triumphs [17,18], from the prediction and observation of the expansion of the universe to the prediction and observation of gravitational waves and black holes [19,20]. In the appendix, we briefly describe some of its classical tests.

Frame-dragging, briefly described in the next section 3, is the phenomenon whereby a current of mass-energy, such as a rotating mass (e.g., the Earth) changes the spacetime geometry and produces a field which affects orbits around the mass [21,22]. It was the object of the GP-B experiment, [23] which flew a drag-free satellite aligned with a guide star. GP-B was launched on 20 April 2004 and had a duration of 17 months, but final results were only delivered in May 2011.The orbit was polar circular, with semimajor axis 7,027.4 km (altitude about 645 km). The satellite carried four 1.9 cm radius quartz spheres, each with a thin coating of niobium. Cryogenics lowered the temperature, so the niobium became superconducting, giving the spheres a magnetic moment, which allowed readout of their direction. In a polar orbit the geodetic precession (spacetime is not flat), and frame dragging act at right

Table 1 Mean of the orbital elements of LARES 2 and LAGEOS over 127 days and the estimated corresponding error in measuring frame-dragging due to the Earth even zonal harmonics

	Mean orbital inclination	Mean semimajor axis	Mean eccentricity
LARES 2	70.1615°	12266.1359395 km	0.00027
LAGEOS	109.8469°	12270.020705 km	0.00403
Deviation of LARES 2 from the optimal orbit	Sum of the two satellites' inclinations – 180° ≅ 0.0084°	Difference of the two satellites' semimajor axes ≅ 3.88477 km	
Error in the test of frame-dragging due to deviations from the optimal orbit	Less than 0.006%	Less than 0.02%	

angles. So, both could be read out simultaneously from the gyros. GP-B determined the geodetic precession to approximately 0.28%, but due to unexpected charge patches on the spheres, the error in the frame dragging was of order of 19% [23] (the geodetic precession is about 170 times the frame dragging rate). Previous work [24] on the orbits of LAGEOS and LAGEOS-2 had given an estimate of frame dragging to approximately 10%, with a disputed challenge which would lead to O(30%) [25]. In [26], an improved test using a longer period of data for the LARES and LAGEOS satellites led to a far improved estimate of frame dragging: the result is the Einstein prediction with an estimated relative error of about 2%.

In spite of all the above experimental and theoretical triumphs of GR, the deterministic physical theory of GR is incompatible with the other fundamental probabilistic physical theory, quantum mechanics. GR predicts the occurrence of spacetime singularities where time ends, every known physical theory ceases to be valid and the spacetime curvature diverges [20]. Recent results [27,28] suggest that a holographic encoding of the formation of a black hole in its surface as it forms can be retrieved as it undergoes evaporation at very late times through Hawking radiation. But for astrophysical black holes these would be *very* late times, far, far exceeding the current age of the universe.

There are other tensions: In cosmology, observations of distant supernovae show mysterious and unexpected accelerated expansion of the universe [29,30]. A possible explanation for this enigmatic result is the *cosmological constant* introduced by Einstein to avoid a dynamical universe, later abandoned by Einstein himself. While the cosmological constant corresponds to vacuum energy (dark energy), to explain the accelerated expansion of the universe, more than 70% of our universe should be composed of dark energy. But dark energy's real nature is a riddle; another tension arises: naive quantum field theory predicts that the vacuum energy should have a value approximately 10^{122} times larger than the dark energy density observed in the universe. Possible explanations include various modifications and extensions of Einstein's gravitational theory, such as the so-called f(R) theories and a time dependent vacuum energy with the exotic name of quintessence [31,32].

3 Dragging of inertial frames

What is "Dragging of inertial frames", or "frame-dragging" [21,22] as Einstein named it in 1913 [14]?

Frame-dragging is an intriguing phenomenon affecting inertial frames with relevant effects in a number of spectacular astrophysical phenomena. In Einstein's theory of general relativity, the inertial frames are *local*, as described by the medium-strong form of the equivalence principle at the foundation of metric theories of gravitation (described by a symmetric metric tensor). Indeed, the equivalence principle states that in a sufficiently small neighborhood of a spacetime event and in the local inertial frames, the gravitational field is locally 'unobservable' and all the non-gravitational laws of physics are the laws of Special Relativity. The strong form of the equivalence principle, a cornerstone of general relativity, includes gravitation itself in the local laws of physics, meaning that an external gravitational field cannot be detected in a local freely falling frame by its influence on local gravitational phenomena [14,15]. One implication of this is that the negative gravitational self-energy of a body contributes to its total gravitational mass.

Local inertial frames are freely falling non-rotating frames whose axes are determined by sufficiently small freely falling test-gyroscopes, realized for example by spinning tops [21,22].

But what do we mean by "non-rotating"? We do not mean non-rotating with respect to the distant stars, i.e., to some asymptotic inertial frame! Indeed, contrary to classical mechanics, the axes of the local inertial frames, i.e., the gyroscopes (sufficiently small mass currents in a loop) are dragged by the external mass-energy currents and can thus rotate with respect to the distant stars. Then any observer fixed with the gyroscopes, even though rotating with respect

to the distant stars, would feel no fictitious or centrifugal force. This intriguing phenomenon that an observer can rotate with respect to the distant stars and at the same time not feel any centrifugal force, is well represented in the movie "Interstellar" where a planet has a complete rotation, with respect to very distant observers and to a nearby huge rotating black hole, in a tenth of a second without being destroyed by the centrifugal forces and without the observers on the planet feeling any centrifugal force at all [33]. The reason being that the planet is rotating (with respect to the distant stars) at exactly the same angular velocity as the local inertial frames which are dragged at such angular velocity by the rotation of the nearby huge rotating black hole of 100 million solar masses.

In gravitation, the dragging of a gyroscope, and of a local inertial frame, is formally similar to the Larmor precession in electrodynamics of a magnetic dipole (magnetic needle formed by local electric currents in a loop) which is "dragged" by an external electric current [34]. This is the well-known phenomenon of the magnetic needle changing orientation due to the Earth's internal electric currents. But in gravitation the gyroscopes have a very special importance since they determine the local inertial frames in which an observer does not feel any centrifugal forces. In Table 2, we compare frame-dragging on a gyroscope and on the orbit of a test-particle (the Lense–Thirring effect [35]) with the Larmor precession of classical electrodynamics.

The dragging of inertial frames has also a formal interesting analogy between the Einstein–Hilbert field equations, in weak-field and slow-motion, and the Maxwell equations [21,22] in electrodynamics. Frame-dragging has some relation to Mach's principle which states that the fictitious and centrifugal forces are due to the rotation with respect to all the masses of the universe [14–16]. Furthermore, frame-dragging is related to interesting and mysterious phenomena in the flow of time around a rotating body. The rotating body could be a spinning black hole or even a rotating cosmology. In the Gödel rotating cosmological model [16], there are closed time-like curves which an observer could follow to go back in time. And, it has a key role in the emission of gravitational waves by the coalescence of two black holes to form a rotating black hole [19] and in the constant orientation of the spectacular jets of plasma from galactic nuclei and quasars, always pointing toward the same direction over emission times which may reach millions of years [21].

4 The LARES 2 space experiment

As reported in Sect. 2, tests of frame-dragging have been carried out with a few percent accuracy using the satellites LARES, LAGEOS and LAGEOS 2 [26]. LARES 2 is designed to improve the test of frame-dragging by at least an order of magnitude [1–4]. Figure 2 displays the concept of the LARES 2 space experiment to accurately measure Earth frame-dragging.

The well-known theorem of conservation of angular momentum in classical mechanics shows that the orbital plane of a test particle has a constant orientation for motion under a central force. Thus, the orbital plane, and the nodal line, of a satellite provide a gyroscope in the gravitational field of a perfectly spherically symmetric body. The nodal line is the intersection of the plane of the orbit with the equatorial plane of the central object. Nevertheless, even in classical mechanics, if the distribution of mass of the central body is not spherically symmetric, the orbital plane, and the nodal line, of a satellite have a shift. In particular, there is a *secular* drift of the node of a satellite due to the even zonal harmonics of the central body [12]. In the spherical harmonic expansion of the gravitational potential of a body, the even zonal harmonics are those of even degree and zero order, i.e., they represent the axially symmetric deviations from spherical symmetry of the gravitational potential, which are also symmetric with respect to the equatorial plane of the body [12].

The non-relativistic nodal drift of two satellites with supplementary inclinations, and with the same semimajor axis, is equal and opposite. So by properly adding the two secular nodal shifts, it will be possible to eliminate the dominant classical shift and to accurately measure the general relativistic node shift. Indeed, the dragging of inertial frames produces the same nodal shift, both in magnitude and sign, on both satellites, independently of their inclination and in the same sense of the Earth's rotation. Hence by properly adding the shift of the nodes of the two satellites we achieve a measurement which is purely the frame dragging. In the previous Section 3 we briefly described this somehow mysterious phenomenon of General Relativity and the Lense–Thirring effect [35]. In weak-field and slow-motion, the Lense–Thirring effect describes the nodal drift of a test-particle due to frame-dragging. For two satellites with supplementary inclinations, the elimination of the bias due to the even zonals in the test of frame-dragging is clearly shown by the well-known equation for the secular nodal drift of a satellite due to the even zonals [12]. The even zonals are the only gravitational perturbations, other than the frame-dragging, which produce secular changes on the node of a satellite. In particular, the largest nodal drift of an Earth satellite is by far due to the even zonal harmonic of degree two, the Earth quadrupole moment. The Earth's even zonals are accurately measured by a number of techniques, including the joint NASA and DLR space missions GRACE (Gravity Recovery and Climate Experiment) and GRACE Follow-On [36,37]. Nevertheless, since even a tiny uncertainty produces a systematic bias in the measurement of frame-dragging, the supplementary inclination

Table 2 Frame-dragging of a gyroscope and of a test particle, and the Larmor precession of a classical dipole moment in a magnetic field B

Frame-dragging $\dot{\Omega}$ of a gyroscope at position x due to the angular momentum $\mathbf{J}$ of a central body (G is the gravitational constant and c the speed of light).	$\dot{\Omega} = \frac{-2G(\mathbf{J}+3(\mathbf{J}\cdot\hat{x})\hat{x})}{c^2\lvert\mathbf{x}\rvert^3}$
Lense–Thirring effect, i.e., frame-dragging of the orbital plane of a test-particle due to the the angular momentum $\mathbf{J}$ of a central body. $\dot{\Omega}$ is the rate of change of the nodal longitude of the test-particle, a its semimajor axis and e its orbital eccentricity.	$\dot{\Omega} = \frac{2G\mathbf{J}}{c^2a^3(1-e^2)^{\frac{3}{2}}}$
Larmor precession $\dot{\Omega}$ of a classical (non-quantum) dipole moment of a current loop of a particle of charge q and mass m in a magnetic field B.	$\dot{\omega} = \frac{-q\mathbf{B}}{2mc}$

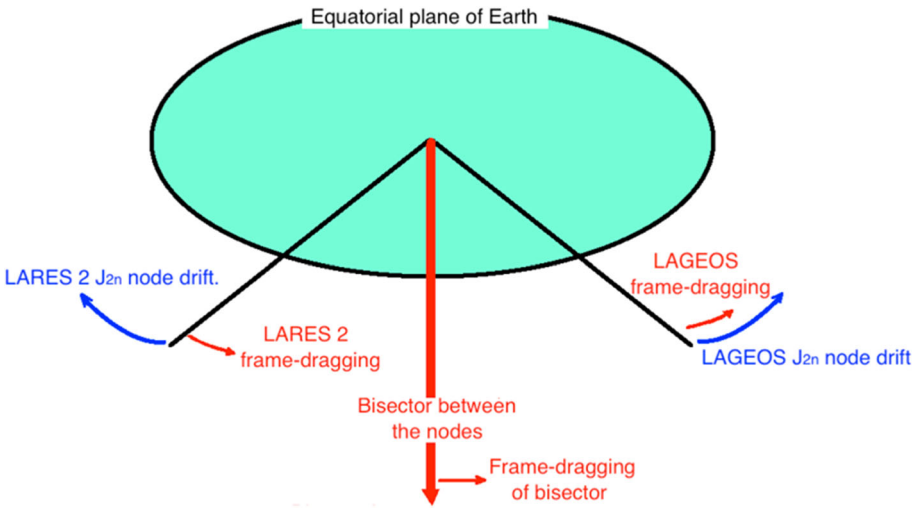

Fig. 2 The concept of the LARES 2 space experiment to accurately test frame-dragging. In this figure is represented the drift of the nodal lines of LARES 2 and LAGEOS. The secular drift, due to the Earth's even zonal harmonics, is equal and opposite for these two satellites with supplementary inclinations. However, frame-dragging produces a drift of their nodal lines which is the same for both satellites, both in magnitude and sign, in the same sense of rotation of the Earth, independently of their inclination. Thus, the bisector of the nodal lines of LARES 2 and LAGEOS is not affected by the Earth's even zonal harmonics and has only a secular drift due to frame-dragging [5], as if it were a huge gyroscope in the gravitational field of a spherically symmetric body

configuration of LARES 2 and LAGEOS effectively allow elimination of such a systematic bias.

LARES 2 will also provide other tests of fundamental physics and general relativity, such as tests of the weak equivalence principle with previously untested materials [38]. The weak equivalence principle, at the foundation of viable theories of gravitation, states that the motion of any test particle due to the gravitational interaction with other bodies is independent of the mass, composition and structure of the particle (see Sect. 2).

Finally, LARES 2 will provide relevant determinations in space geodesy and geodynamics. It will improve the definition of the International Terrestrial Reference Frame (ITRF) by contributing to a more accurate determinations of the Earth's center of mass. It will also provide more accurate models of the Earth gravitational field.

Based on our previous error analyses [1–4, see also 5–11] and given the almost perfectly supplementary orbits of LARES 2 and LAGEOS, we estimate that over a sufficiently long period of time, we may reach an accuracy of about 0.2%, or less in the frame-dragging measurement (see Table 3).

5 The LARES 2 structure

The main characteristic of a passive geodetic satellite is its low cross-sectional-area to mass ratio that allows reconstruction of the orbit as due to gravity only. This permits very accurate tests of general relativity, but it is also important for Earth's science and in particular for monitoring of global climate changes [39]. In fact, global warming caused mass redistribution, for instance ice melting on south pole and on

Table 3 Relative errors in the LARES 2 measurement of frame-dragging

Source of error	Estimated error
Even zonal harmonics and injection error	Less than 0.1% of frame-dragging
Non-zonal harmonics and tides	$\cong$ 0.1% of frame-dragging
Albedo	$\cong$ 0.1% of frame-dragging
Thermal drag and satellites eclipses	$\cong$ 0.1% of frame-dragging
Measurement error of the LAGEOS and LARES 2 orbital parameters	$\cong$ 0.1% of frame-dragging
Total RSS Error	$\cong$ 0.2% of frame-dragging

Greenland's ice sheet affects the gravity field of Earth and thus the satellite orbit.

Similarly to LARES, the LARES 2 satellite has been designed to minimize the cross-sectional-area to mass ratio, i.e., the forces acting on the surface of the satellite, such as the solar radiation pressure and the atmospheric drag. The two main constraints for the LARES 2 design were the maximum mass allowed by the launch vehicle and the minimum diameter necessary for sufficient reflected power at the laser ground stations. Starting with a study performed with the LARES experimental laser-ranging data [40], the final diameter of LARES 2 was set to 424 mm. This value was chosen by taking into account two factors: first the need to increase the satellite diameter from the 364 mm of LARES satellite, since the much higher altitude of LARES 2 reduces returned photons count, and second the different type of Cube Corner Retroreflectors (CCR) used on LARES 2. Comparison of tests performed on the custom made 1.5 in. diameter retroreflectors of LARES [41,42] confirmed their expected higher optical cross-section compared to the 1 in. Commercial Off The Shelf (COTS) retroreflectors used on LARES 2. However, that is compensated by the much higher number of CCRs on LARES 2 (Table 4). In Fig. 3 is reported the Far Field Diffraction Pattern of a 1 in. COTS CCR from which we have evaluated the optical cross-section. The decision to use COTS retroreflectors was taken after the optical tests performed on a sample of 10 CCRs demonstrated their good quality in terms of surface flatness ($\frac{\lambda}{10}$ for back face and $\frac{\lambda}{4}$ for the front face, with λ being the laser light wavelength) and dihedral angle accuracy. The size of the chosen CCRs was reduced to 1 in. on LARES 2 for two reasons. The first one concerns the CCR Far Field Diffraction Pattern (FFDP) which is constituted by laser light patches arranged in rings whose diameter is related to the CCR front face diameter d (Fig. 3). The first dark ring angular position is at about $1.2\frac{\lambda}{d}$ and the CCR diameter of 1 in. is almost perfect to avoid the ground station being at the dark ring of the FFDP. The second reason is that for a smaller CCR it is easier to maintain the surface quality and to have a reduced number of volume defects that could darken the CCR, in the decades to come, due to the interaction of the defects with UV sunlight.

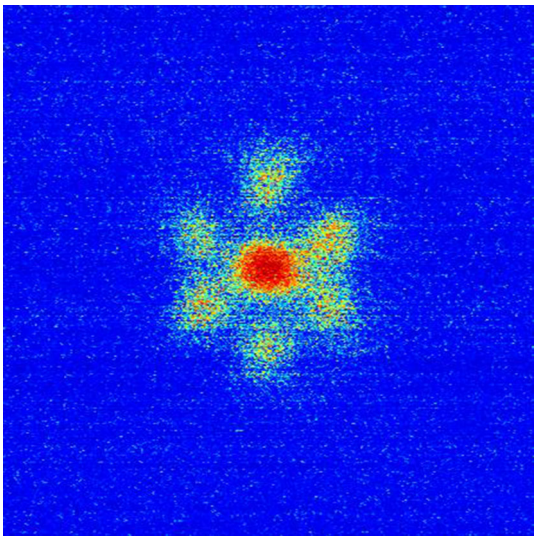

Fig. 3 FFDP of a 1 in. CCR, heated at 70 °C, during a thermovacuum test. Blue corresponds to no energy, red to maximum energy, other colours to intermediate energy

The number of CCRs on LARES 2 is much higher than on LARES for several reasons. The most obvious one is that the CCRs have a front face diameter of 1 in. instead of 1.5 in. The second reason is that the increased diameter of the satellite allows to mount more CCRs. The third one is that the packing of the CCR is more effective on LARES 2: its CCR density is higher because of the special CCR distribution. In fact, the classical ordered distribution of CCRs by rows, or parallels, typically used on passive geodetic satellites, has been abandoned on LARES 2 in favour of random-like one. The CCRs have been placed in positions given by the best known solution of Thomson's problem which seeks the minimum of the Coulomb potential of classical electrons constrained on a spherical surface. However, the real distribution had to be slightly changed to accommodate the interfaces of the separation system. The LARES 2 separation system is derived from the LARES separation system design [43] and has four hemispherical cavities along the equator of the satellite and some contact areas at the south pole of the satellite. After an intense experimental trade-off study [44] on the custom and commercial alloys with a density in the range of 8200–9000 kg/m^3 and with mechanical and surface hardness character-

Table 4 Characteristics of the LARES 2 satellite compared to LARES and to the LAGEOS satellites (cross-sectional area = πR^2)

Satellite	Material alloys	Radius, R (m)	Mass (kg)	Cross-sectional area (m^2)	Cross-sectional area over mass	Cross-sectional area over mass relative to LAGEOS	CCR size (in.)	Number of CCRs	Optical cross-section (10^6 m^2)
LARES	Tungsten	0.182	386.8	0.1041	0.00026913	0.3875	1.5	92	3.3 (theory)
LARES 2	Nickel	0.212	294.8	0.1412	0.00047897	0.6896	1	303	2.7
LAGEOS	Aluminum and brass	0.300	407	0.2827	0.00069459	1	1.5	426	7
LAGEOS 2	Aluminum and brass	0.300	405.4	0.2827	0.00069734	1.0039	1.5	426	7

istics capable of withstanding the forces by the separation system arms and pushing spring, the final decision was to use the commercial nickel superalloy Inconel 718.

6 Conclusions

Thanks to the extremely high injection precision of LARES 2 into an orbit with supplementary inclination to that of the LAGEOS satellite, the accurate determination of the Earth's gravitational field by GRACE and GRACE Follow-On, and the special design of the satellite, LARES 2 will provide very accurate tests of frame-dragging, a relevant and intriguing prediction of Einstein's theory of general relativity. The tests of frame-dragging with LARES 2 and LAGEOS are designed to reach an accuracy of a few parts in a thousand. LARES 2 will also provide other tests of fundamental physics and general relativity and improved determinations in space geodesy and geodynamics.

Acknowledgements The authors wish to thank the Italian Space Agency for supporting the LARES and LARES 2 missions under the Agreements 2020-7-HH.0 and 2017-23-H.0, the European Space Agency for providing the VEGA C inaugural flight, Avio for its support to the missions and the International Laser Ranging Service for tracking the satellites and providing the laser ranging data. E.C. Pavlis acknowledges the support of NASA Grant 80NSSC22M0001 and computational resources provided by NASA's High-End Computing (HEC). The authors would also like to thank the anonymous referees for valuable comments that improved the quality of the paper.

Data Availability Statement The Satellites Laser Ranging (SLR) data are availbale at the NASA CDDIS (Crustal Dynamics Data Information System).

Funded by SCOAP^3. SCOAP^3 supports the goals of the International Year of Basic Sciences for Sustainable Development.

Appendix: Some tests of general relativity

Accurate tests [17,18] of GR include the perihelion precession of Mercury, and the periastron advance of an orbiting body, the equivalence principle [45] and the time-dilation of clocks in a gravitational field [46], the deflection and time-delay of electromagnetic waves by a mass [47], the dynamics

of the Moon, accurately measured by Lunar Laser Ranging (LLR) [48] and of binary pulsars [49], gravitational lensing and other astrophysical observations. Gravitational waves have been indirectly observed in agreement with the prediction of GR from the rate of change of the orbital period of the binary pulsar PSR B1913 + 16 [49]. And the LIGO advanced detectors (Caltech and MIT), together with the Virgo and the KAGRA detectors, have directly detected the gravitational waves from the merger of black holes and/or neutron stars [19].

GR was introduced by Einstein in 1915/1916. He was motivated by the theoretical question of making a gravitational theory which was compatible with special relativity, and in fact GR "contains" special relativity and reduces to special relativity when gravitational fields are vanishingly weak. Of course, the question arose of experimental validation. When Einstein wrote, only three experiments seemed feasible: (a) measurement of the redshift, (b) measurement of the deflection of light, and (c) measurement of the precession of the perihelion in planetary orbits.

(a) General relativity predicts that defined-frequency light (e.g., a particular spectral line of iron), emitted near a massive body (i.e., deep in its gravitational well), arrives at an observer far from the massive body redshifted, i.e., its wavelength is longer (it is redder) than the same line produced locally by the observer. This is not a classical Doppler effect; the source and observer are at rest with respect to one another. Initial efforts to detect the effect in local stars (e.g., the Sun) were ambiguous because of large turbulent motions on the Sun's surface led to Doppler broadening of the lines so that the $\approx 10^{-8}$ predicted fractional shift was washed out. Not until experiments by Pound & Rebka [50] and Pound & Snider [51] was an accurate validation achieved, using γ-rays emitted by Co-57 and absorbed in Fe-57, with a fractional uncertainty $8 \cdot 10^{-3}$ of the total $5 \cdot 10^{-15}$ predicted relative redshift for a 22.5 meter elevation difference. On June 18, 1976, a redshift experiment [46] was launched on a *Scout* rocket to an altitude of approximately 10,000 *km*. Microwave links found the expected redshift to parts $\approx 7 \cdot 10^{-5}$. Chou et al. [52] used optical clocks separated in altitude by 33 cm to measure the expected redshift. And, of course, GNSS systems like Galileo and GPS continuously validate the Relativistic prediction [53].

(b) The earliest efforts to measure the deflection of light were photographic efforts during solar eclipses when stars were visible near the (blocked-out) Sun. They definitely showed the effect, but with large errors. Radio astronomy allows continuous monitoring of the position of radio sources as they "pass near" the Sun; deflection can be measured at very large angles from the Sun; the Hipparcos astrometric (optical) satellite similarly solved over the whole celestial sphere for solar deflection. And lensing is ubiquitous in deep "dark field" images from space telescopes.

(c) In the solar system, only Mercury has a relativistic perihelion precession that is reasonably observable by optical techniques. Prior to Einstein's discovery of GR, Mercury had a known anomalous perihelion precession of about 43 seconds of arc per century, close to the relativistic prediction. Regular observation of the Hulse–Taylor binary pulsar [49] is completely described by GR and shows periapse precession of 4.2° degrees per year.

We also briefly report some of the new tests of GR. Special relativity gives us the well-known relation $E = mc^2$; energy and mass are essentially the same thing. The fundamental principle underlying GR is the Equivalence Principle [14,15], which states that test bodies fall the same way in a gravitational field, regardless of composition (Weak Equivalence), or regardless of composition and percentage of gravitational binding energy (Strong Equivalence). Implied is also the statement that gravitational active and gravitational passive mass are the same. The *MICROSCOPE* satellite experiment [45] compared the behavior of concentric cylinders of titanium and platinum, and found no difference from Equivalence Principle behavior to parts in 10^{15}. In [38] satellites of different materials and at different semimajor distances (in low eccentricity orbits) were compared: LARES, made of an alloy of sintered tungsten, semimajor axis $\sim$ 7820 km, and LAGEOS and LAGEOS-2, made of brass and aluminum, semimajor axis $\sim$ 12,200 km. It was found that the observed orbits satisfied the GR predictions to relative errors $O(10^{-9})$. Note that this test included a verification of Earth's gravitational field $O(r^{-2})$.

References

1. I. Ciufolini, A. Paolozzi, E.C. Pavlis, G. Sindoni, R. Koenig, J.C. Ries, R. Matzner, V. Gurzadyan, R. Penrose, D. Rubincam, C. Paris, A new laser-ranged satellite for general relativity and space geodesy. I. Introduction to the LARES 2 space experiment. Eur. Phys. J. Plus **132**, 336 (2017). https://doi.org/10.1140/epjp/i2017-11635-1
2. I. Ciufolini, E.C. Pavlis, G. Sindoni, J.C. Ries, A. Paolozzi, R. Koenig, C. Paris, A new laser-ranged satellite for general relativity and space geodesy. II. Monte Carlo simulations and covariance analyses of the LARES 2 experiment. Eur. Phys. J. Plus **132**, 337 (2017). https://doi.org/10.1140/epjp/i2017-11636-0
3. I. Ciufolini, R. Matzner, V. Gurzadyan, R. Penrose, A new laser-ranged satellite for general relativity and space geodesy. III. De Sitter effect and the LARES 2 space experiment. Eur. Phys. J. C **76**, 120 (2016). https://doi.org/10.1140/epjc/s10052-016-3961-8
4. I. Ciufolini, R.A. Matzner, J.C. Feng, A. Paolozzi, D.P. Rubincam, E.C. Pavlis, J.C. Ries, G. Sindoni, C. Paris, A new laser-ranged satellite for general relativity and space geodesy: IV. Thermal drag and the LARES 2 space experiment. Eur. Phys. J. Plus (2018). https://doi.org/10.1140/epjp/i2018-12174-y
5. I. Ciufolini, Measurement of the LenseThirring drag on high-altitude laser-ranged artificial satellites. Phys. Rev. Lett. **56**, 278–281 (1986). https://doi.org/10.1103/PhysRevLett.56.278

6. I. Ciufolini, A comprehensive introduction to the LAGEOS gravimetric experiment. Int. J. Mod. Phys. A **4**, 3083–3145 (1989). https://doi.org/10.1142/S0217751X89001266
7. B. Tapley, J.C. Ries, R.J. Eanes, M.M. Watkins, NASA-ASI Study on LAGEOS III, CSR-UT publication n. CSR-89-3, Austin, Texas (1989)
8. I. Ciufolini et al., *ASI-NASA Study on LAGEOS III* (CNR, Rome, Italy, 1989)
9. I. Ciufolini, *Theory and Experiments in General Relativity and other Metric Theories, PhD Dissertation* (Univ. of Texas, Austin, 1984)
10. J.C. Ries, *Simulation of an experiment to measure the LenseThirring precession using a second LAGEOS satellite, PhD Dissertation* (Univ. of Texas, Austin, 1989)
11. G.E. Peterson, *Estimation of the LenseThirring Precession Using Laser-Ranged Satellites, PhD Dissertation* (Univ. of Texas, Austin, 1997)
12. W.M. Kaula, *Theory of Satellite Geodesy* (Blaisdell, Waltham, 1966)
13. M.R. Pearlman, C.E. Noll, E.C. Pavlis, F.G. Lemoine, L. Combrink, J.J. Degnan, G- Kirchner, U. Schreiber, The ILRS: approaching 20 years and planning for the future. J. Geodesy **93**, 2161–2180 (2019). https://doi.org/10.1007/s00190-019-01241-1
14. C.W. Misner, K.S. Thorne, J.A. Wheeler, *Gravitation* (Freeman, San Francisco, 1973)
15. S. Weinberg, *Gravitation and Cosmology: Principles and Applications of the General Theory of Relativity* (Wiley, New York, 1972)
16. I. Ciufolini, J.A. Wheeler, *Gravitation and Inertia* (Princeton University Press, Princeton, 1995)
17. C.M. Will, *Theory and Experiment in Gravitational Physics*, 2nd edn. (Cambridge University Press, Cambridge, 1993)
18. S. Turyshev, Experimental tests of general relativity: recent progress and future directions. Phys. Usp. **52**, 1–27 (2009). https://doi.org/10.3367/UFNe.0179.200901a.0003
19. B.P. Abbott et al., (LIGO Scientific and Virgo Collaborations), Tests of general relativity with GW150914. Phys. Rev. Lett. **116**, 221101 (2016). https://doi.org/10.1103/PhysRevLett.116.221101
20. R. Penrose, Gravitational collapse and space-time singularities. Phys. Rev. Lett. **14**, 57–59 (1965). https://doi.org/10.1103/PhysRevLett.14.57
21. K.S. Thorne, R.H. Price, D.A. Macdonald, *The Membrane Paradigm* (Yale University Press, NewHaven, 1986)
22. I. Ciufolini, Dragging of inertial frames. Nature **449**, 7158 (2007). https://doi.org/10.1038/nature06071
23. C.W.F. Everitt et al., Gravity probe B: final results of a space experiment to test general relativity. Phys. Rev. Lett. (2011). https://doi.org/10.1103/PhysRevLett.106.221101
24. I. Ciufolini, E.C. Pavlis, A confirmation of the general relativistic prediction of the Lense–Thirring effect. Nature **431**, 958–960 (2004). https://doi.org/10.1038/nature03007
25. J. Ries, I. Ciufolini, E. Pavlis, A. Paolozzi, R. Koenig, R. Matzner, G. Sindoni, H. Neumayer, The Earth frame-dragging via laser ranged satellites: a response to "some considerations on the present day results for the detection of frame-dragging after the final outcome of GP-B" by Iorio L. EPL 96 (2011). https://doi.org/10.1209/0295-5075/96/30002
26. I. Ciufolini, A. Paolozzi, E.C. Pavlis, G. Sindoni, J. Ries, R. Matzner, R. Koenig, C. Paris, V. Gurzadyan, R. Penrose, An improved test of the general relativistic effect of frame-dragging using the LARES and LAGEOS satellites. Eur. Phys. J. C **79**, 872 (2019). https://doi.org/10.1140/epjc/s10052-019-7386-z
27. G. Penington, Entanglement wedge reconstruction and the information paradox. J. High Energy Phys. **2020**, 2 (2020). https://doi.org/10.1007/JHEP09(2020)002
28. A. Almheiri, N. Engelhardt, D. Marolf, H. Maxfield, The entropy of bulk quantum fields and the entanglement wedge of an evaporating black hole. J. High Energy Phys. **2019**, 63 (2019). https://doi.org/10.1007/JHEP12(2019)063
29. S. Perlmutter, Supernovae, dark energy, and the accelerating universe. Phys. Today **56**, 53–60 (2003). https://doi.org/10.1063/1.1580050
30. R.R. Caldwell, Dark energy. Phys. World **17**, 37–42 (2004)
31. T.L. Smith, A. Erickcek, R. Caldwell, M. Kamionkowski, Effects of Chern–Simons gravity on bodies orbiting the Earth. Phys. Rev. D **77**, 024015 (2008). https://doi.org/10.1103/PhysRevD.77.024015
32. A. De Felice, S. Tsujikawa, f(R) Theories. Living Rev. Relativ. (2010). https://doi.org/10.12942/lrr-2010-3
33. K.S. Thorne, *The Science of Interstellar*, WW Norton & (2014)
34. J.D. Jackson, *Classical Electrodynamics* (Wiley, New York, 2021)
35. J. Lense, H. Thirring, Uber den Einfluss der Eigenrotation der Zentralkörper auf die Bewegung der Planeten und Monde nach der Einsteinschen Gravitationstheorie. Phys. Z. 19, 156–163 (1918) [See also English translation by, B. Mashhoon, F.W. Hehl, D.S. Theiss, Gen. Relativ. Gravit. 16, 711–750 (1984)]
36. B.D. Tapley, S. Bettadpur, M. Watkins, C. Reigber, The gravity recovery and climate experiment: mission overview and early results. Geophys. Res. Lett. (2004). https://doi.org/10.1029/2004GL019920
37. F.W. Landerer, F. Flechtner et al., Extending the global mass change data record: GRACE follow-on instrument and science data performance. Geophys. Res. Lett. (2020). https://doi.org/10.1029/2020GL088306
38. I. Ciufolini, R. Matzner, A. Paolozzi, E.C. Pavlis, G. Sindoni, J. Ries, V. Gurzadyan, R. Koenig, Satellite laser-ranging as a probe of fundamental physics. Sci. Rep. **9**, 15881 (2019). https://doi.org/10.1038/s41598-019-52183-9
39. G. Sindoni, C. Paris, C. Vendittozzi, E.C. Pavlis, I. Ciufolini, A. Paolozzi, The contribution of LARES to global climate change studies with geodetic satellites. ASME 2015 Conference on Smart Materials, Adaptive Structures and Intelligent Systems, SMASIS 2015, 2015, 2. https://doi.org/10.1115/SMASIS2015-8924
40. E. C. Pavlis, A. Paolozzi, C. Paris, I. Ciufolini and G. Sindoni, Quality assessment of LARES satellite ranging data: LARES contribution for improving the terrestrial reference frame, 2nd IEEE International Workshop on Metrology for Aerospace, MetroAeroSpace 2015-Proceedings, 2015, pp. 1–5, 7180616. https://doi.org/10.1109/MetroAeroSpace.2015.7180616
41. C. Paris, R. Neubert, Tests of LARES and CHAMP cube corner reflectors in simulated space environment. IEEE Aerospace Conference Proceedings, 2015, 2015-June, 7119150. https://doi.org/10.1109/AERO.2015.7119150
42. A. Paolozzi, I. Ciufolini, L. Schirone, D. Spano, G. Sindoni, C. Vendittozzi, G. Battaglia, M. Ramiconi, Tests of lares cube corner reflectors in simulated space environment (preliminary results), 61st International Astronautical Congress 2010. IAC **2010**(9), 7390–7396 (2010)
43. C. Paris, Vibration tests on the preloaded LARES satellite and separation system. Aerosp. Sci. Technol. **42**, 470–476 (2015). https://doi.org/10.1016/j.ast.2015.01.023
44. A. Paolozzi, G. Sindoni, F. Felli, D. Pilone, A. Brotzu, I. Ciufolini, E.C. Pavlis, C. Paris, Studies on the materials of LARES 2 satellite. J. Geodesy **93**(11), 2437–2446 (2019). https://doi.org/10.1007/s00190-019-01316-z
45. P. Touboul et al. (MICROSCOPE Collaboration), MICROSCOPE Mission: Final Results of the Test of the Equivalence Principle. Phys. Rev. Lett. 129, 121102 (2022). https://doi.org/10.1103/PhysRevLett.129.121102
46. R.F.C. Vessot, M.W. Levine, E.M. Mattison, E.L. Blomberg, T.E. Hoffman, G.U. Nystrom, B.F. Farrel, R. Decher, P.B. Eby, C.R. Baugher, J.W. Watts, D.L. Teuber, F.D. Wills, Test of relativistic gravitation with a space-borne hydrogen maser. Phys. Rev. Lett. **45**, 2081 (1980). https://doi.org/10.1103/PhysRevLett.45.2081

47. S. Shapiro, J. Davis, D. Lebach, J. Gregory, Measurement of the solar gravitational deflection of radio waves using geodetic very-long-baseline interferometry data, 1979–1999. Phys. Rev. Lett. **92**, 121101 (2004). https://doi.org/10.1103/PhysRevLett.92.121101
48. J.G. Williams, S.G. Turyshev, D.H. Boggs, Progress in lunar laser ranging tests of relativistic gravity. Phys. Rev. Lett. **93**, 261101 (2016). https://doi.org/10.1103/PhysRevLett.93.261101
49. R.A. Hulse, J.H. Taylor, Discovery of a pulsar in a binary system. Astrophys. J. **195**, L51–L53 (1975). https://doi.org/10.1086/181708
50. R.V. Pound, G.A. Rebka, Gravitational red-shift in nuclear resonance. Phys. Rev. Lett. **3**(9), 439–441 (1959). https://doi.org/10.1103/PhysRevLett.3.439
51. R.V. Pound, J.L. Snider, Effect of gravity on gamma radiation. Phys. Rev. **140**(3B), B788–B803 (1965). https://doi.org/10.1103/PhysRev.140.B788
52. C.W. Chou, D.B. Hume, T. Rosenband, D.J. Wineland, Optical clocks and relativity. SCIENCE Vol 329. pp. 1630–1633 (24 Sep 2010). https://doi.org/10.1126/science.1192720
53. P. Delva, N. Puchades, E. Schönemann, F. Dilssner, C. Courde, S. Bertone, F. Gonzalez, A. Hees A, C. Le Poncin-Lafitte, F. Meynadier, R. Prieto-Cerdeira, Gravitational redshift test using eccentric Galileo satellites. Phys. Rev. Lett. **121**(23), 231101 (2018). https://doi.org/10.1103/PhysRevLett.121.231101